FOREWORD

This report was prepared by Midwest Research Institute under USAF Contract No. AF 33(616)-7058. The contract was initiated under Project No. 7360, "The Chemistry and Physics of Materials," Task No. 736002, "Nondestructive Methods." The work was administered under the Directorate of Materials and Processes, Deputy for Technology, Aeronautical Systems Division, with Mr. R. R. Rowand acting as project engineer.

This report covers work conducted from 1 February 1961 to 31 January 1962.

The work was performed under the direction of Mr. Fred Rollins, Jr. Personnel directly involved in prosecution of the research have been Messrs. Jerry Jones, Donald Kobett, Neil Abbott, James Gravitt, Paul Gutshall, and Phillip James.

ABSTRACT

The study of stress-induced birefringence has been continued in both polycrystalline and single crystal experiments. The effect is explained on the basis of nonlinear elasticity theory. Experiments indicate that dislocation activity does not strongly affect results in polycrystalline specimens, however, a pronounced influence may be observed in single crystals.

Nonlinear elasticity theory has been used to investigate the interaction of two intersecting, plane, elastic waves in a homogeneous, isotropic medium. A criterion for the occurrence of a strong scattered wave has been derived. The criterion is formulated as a relationship between the second order elastic constants of the material, the angle between the intersecting wave vectors, and the ratio of primary wave frequencies. The amplitude of the scattered wave is found to be proportional to the volume of interaction and dependent on the third order elastic constants of the material. Preliminary efforts to experimentally verify the theoretical predictions are described.

This report has been reviewed and is approved.

W. J. TRAPP
Chief, Strength and Dynamics Branch
Metals and Ceramics Laboratory
Directorate of Materials and Processes

TABLE OF CONTENTS

I. INTRODUCTION

In recent years considerable effort has been directed toward the detection and measurement of residual stresses. Most of the methods that have been successfully developed are destructive or semidestructive in nature. These methods, in general, are based on the fact that relieving the stresses will alter the dimensions of the body. Successive sections of the test piece are removed by chemical or mechanical means and the strain relaxation that occurs in the remaining material is measured. The stress distribution is then calculated from the strain distribution found in the metal specimen.

The only nondestructive method that is successfully used in measuring residual stresses is one which utilizes X-ray diffraction techniques. Even this method has a number of disadvantages. Good accuracy is obtained only with specimens that yield sharp diffraction lines. Quenched steels or cold worked metals give diffuse lines that produce very large errors. An even greater limitation is that only surface stresses can be investigated using this method.

During the past two years Midwest Research Institute has been engaged in a study of the stress-dependent aspects of ultrasonic propagation in solid materials. It is hoped that the results of this study may facilitate the application of ultrasonics to specific residual stress problems. An earlier report[1] covers the first year's work and should be consulted for experimental details that have been intentionally omitted in the following discussion.

II. STRESS-INDUCED BIREFRINGENCE

A. General Discussion

It has been recognized for some time that the velocity and attenuation of ultrasonic waves traveling through solid materials are usually stress-dependent. The exact nature of these stress-dependent changes is not completely understood but recent advances in dislocation theory and finite elasticity can explain many of the experimental observations.

A property that we have studied in several solids is the stress-induced double refraction of megacycle shear waves. In a rectangular coordinate

Manuscript released by authors February 1962 for publication as a WADD Technical Report.

system, let us consider a shear wave traveling in the x-direction. If the material is isotropic, we will find that the shear wave velocity is independent of the direction of particle motion. However, if we remove the isotropy by applying a tensile stress in the y-direction, the velocity is found to vary with the direction of particle motion. Under these conditions it is impossible to propagate a plane polarized shear wave except when the particle motion is either parallel or perpendicular to the applied stress. Referring to the above two velocities as V_{S1} and V_{S2} respectively, we can define a fractional velocity difference, $(\Delta V/V) = (V_{S1}-V_{S2})/\bar{V}$, where $\bar{V}$ is an average of V_{S1} and V_{S2}. The value of $\Delta V/V$ can be determined experimentally using a simple pulse-echo technique.[1] It has been well established that the $\Delta V/V$ values are stress-dependent and, in fact, vary linearly with the stress level. The correlation between theory and observation is described in the following two sections.

B. Predictions Based on Theory of Finite Strain

The velocities of longitudinal and shear waves in an isotropic, homogeneous medium are usually given by the following expressions:

$$V_L = \sqrt{\frac{\lambda+2\mu}{\rho}}\ ,\ V_S = \sqrt{\frac{\mu}{\rho}} \qquad (1)$$

where λ and μ are the second order Lamé constants and ρ is the density. These expressions are derived on the basis of infinitesimal deformations. They do not predict a stress-dependent velocity so long as the density remains constant. However, by using the finite strain method of Murnaghan,[2] Hughes and Kelly[3] calculated the velocities of ultrasonic waves in isotropic media and obtained the stress-dependent expression shown below:

(a) For hydrostatic pressure, p

Longitudinal wave
$$\rho_o V_L^2 = (2\mu+\lambda) - \frac{p}{3K}\left[10\mu+7\lambda+6\ell+4m\right] \qquad (2)$$

Shear wave
$$\rho_o V_S^2 = \upsilon - \frac{p}{3K}\left[3(2\mu+\lambda)+3m - \frac{n}{2}\right] \qquad (3)$$

(b) Uniaxial Pressure, P, and wave propagation both in x-direction

Longitudinal wave
$$\rho_o V_L^2 = (2\mu+\lambda) - \frac{P}{3K}\left[\frac{\mu+\lambda}{\mu}(10\mu+4\lambda+4m)+\lambda+2\ell\right] \quad (4)$$

Shear wave
$$\rho_o V_S^2 = \mu - \frac{P}{3K}\left[4(\mu+\lambda) + \frac{\lambda}{4\mu} n + m\right] \quad (5)$$

(c) Uniaxial Pressure, P, in x-direction with wave propagation in y-direction

Longitudinal wave
$$\rho_o V_L^2 = (2\mu+\lambda) - \frac{P}{3K}\left[2\ell - \frac{2\lambda}{\mu}(2\mu+\lambda+m)\right] \quad (6)$$

Shear wave with particle motion in x-direction
$$\rho_o V_{S1}^2 = \mu - \frac{P}{3K}\left[2\mu+\lambda+m+\frac{\lambda}{4\mu} n\right] \quad (7)$$

Shear wave with particle motion in z-direction
$$\rho_o V_{S2}^2 = \mu - \frac{P}{3K}\left[m-2\lambda - \frac{\mu+\lambda}{2\mu} n\right] \quad (8)$$

In these expressions, ρ_o is the density of the undeformed medium, K is the bulk modulus and the terms ℓ, m, and n are referred to as third order elastic constants. The latter give an indication of the nonlinearity in the elastic behavior of a material. It is easily seen that when the hydrostatic pressure or uniaxial stress is zero the expressions all reduce to the two expressions given in (1).

The three third order constants that appear in expressions (2)-(8) can, of course, be determined experimentally by accurately measuring the velocity changes produced in at least three independent cases. It is possible to independently determine the third order constant, n, by a simple technique that does not necessitate the accurate measurement of absolute velocity. When shear waves are sent through a specimen in a direction that is perpendicular to the direction of an applied uniaxial stress, expressions (7) and (8) indicate that the velocity depends upon the particle motion direction. The initially isotropic material becomes birefringent. Pure shear waves can be propagated in this case only when the particle motion is either parallel or

perpendicular to the applied load. If we subtract expression (8) from (7) and remember that $K = 1/3(2\mu+3\lambda)$, we get

$$\rho_o V_{S1}^2 - \rho_o V_{S2}^2 = - \frac{P}{4\mu} \left[4\mu+n\right] \quad . \tag{9}$$

Since $V_{S1} + V_{S2} \cong 2V_o$, we then have

$$V_{S1} - V_{S2} \cong - \frac{P}{8\rho_o V_o \mu} \left[4\mu+n\right] \quad , \tag{10}$$

or expressed as a fractional difference

$$\frac{V_{S1}-V_{S2}}{V_o} = \Delta V/V \cong - \frac{P}{8\rho_o V_o^2 \mu} \left[4\mu+n\right] = - \frac{P}{8\mu^2} \left[4\mu+n\right] \tag{11}$$

From (11) we see that the fractional difference between V_{S1} and V_{S2} is a linear function of the uniaxial stress, P . Note also that experimental determination of $\Delta V/V$ at a given stress is sufficient to evaluate the third order constant, n .

The velocity of ultrasonic waves in single crystals is also stress-dependent, but the velocity expressions are somewhat more involved due to the loss in symmetry. Seeger and Buck[4] have derived the differential equations for wave propagation in cubic crystals that have superimposed finite stresses. There are six third order elastic constants for such crystals and Bateman et al.,[5] have recently used ultrasonic techniques to evaluate all of these constants for germanium. The velocity expression given in Ref. 5 for a shear wave traveling in the [001] direction with particle motion parallel to a [110] pressure is as follows:

$$\rho V_{11} = (1+\gamma+\alpha-\beta)C_{44} + \left[(\alpha+\beta)/4\right] C_{144} + \left[(\alpha+\beta+2\gamma)/4\right] C_{166} + \left[(\alpha-\beta)/4\right] C_{456} \quad . \tag{12}$$

For a shear wave traveling in the same direction but with particle motion perpendicular to $[1\bar{1}0]$, the expression is

$$\rho V_{\perp} = (1+\gamma+\beta-\alpha)C_{44} + [(\alpha+\beta)/4]\, C_{144} + [(\alpha+\beta+2\gamma)/4]\, C_{166} + [(\beta-\alpha)/4]\, C_{456} \cdot \qquad (13)$$

In the above expressions α , β , and γ are all linear functions of the applied stress and the C_{ijk} terms are the third-order moduli. By using the approximation $(V_{\parallel} + V_{\perp}) \cong 2V$, the fractional velocity difference for shear wave propagation in the $[1\bar{0}0]$ direction becomes

$$\frac{V_{\parallel} - V_{\perp}}{V} \cong - \frac{P}{8C_{44}^2} (4C_{44}+C_{456}) \cdot \qquad (14)$$

Here again we see that the fractional velocity difference is a linear function of the uniaxial stress P .

It should be emphasized at this point that the above expressions, (2)-(8) and (12)-(13), were derived for a perfectly elastic material. For most real materials, an applied stress will produce some anelastic strain in addition to the elastic strain. Granato and Lücke[6,7] have developed a theory of energy losses and modulus changes that are due to dislocation damping. The theory is based on the model of a dislocation loop oscillating under the influence of an applied stress. Without going into the details of this theory, it is sufficient to state that the fractional velocity change due to the dislocations is proportional to the dislocation density and the second power of the dislocation loop length. There is considerable experimental evidence that supports the Granato-Lücke theory and there is no question that dislocations do affect the propagation of ultrasonic waves. Additional discussion of this subject may be found in the following section.

C. Experimental Results

The pulse-echo technique[1] has been used to measure stress-induced changes of $(\Delta V/V)$ in a variety of materials. Figure 1 shows some typical curves and confirms the linear relationship between $(\Delta V/V)$ and stress level.

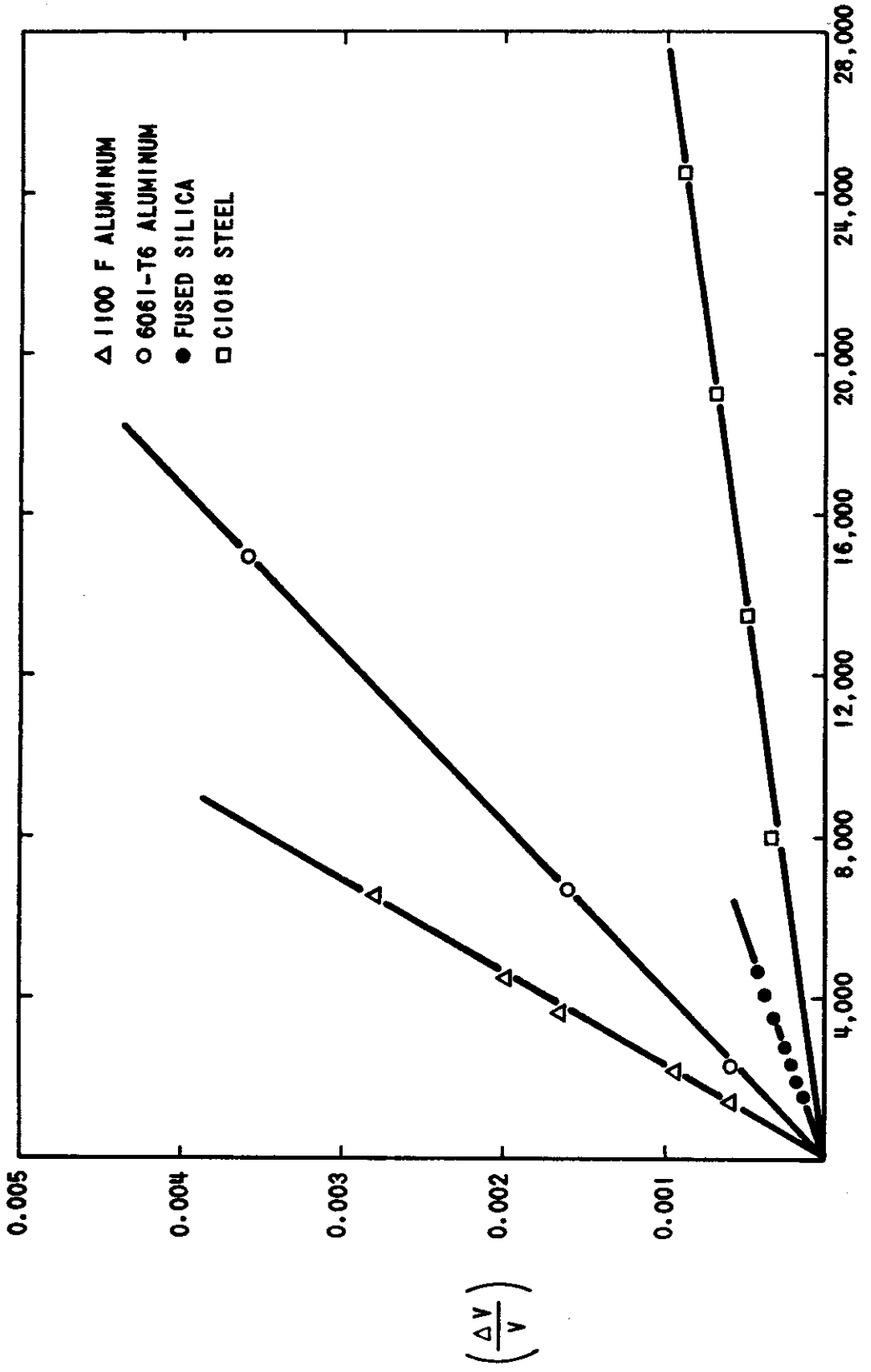

Figure 1 - Stress-Induced Birefringence for Several Materials

It was mentioned previously that the $(\Delta V/V)$ measurements might be used to evaluate the third order elastic constant, n . We see from Eq. (11) that a plot of $(\Delta V/V)$ versus stress should yield a straight line with a slope of $-(4\mu+n)/8\mu^2$. The slopes of the curves shown in Figure 1 have, therefore, been used to calculate n for each material and the results are summarized in Table I.

TABLE I

Material	n (psi)
6061-T6 Aluminum	$-(45.2 \pm 1.8) \times 10^6$
1100-F Aluminum	$-(69.2 \pm 5.5) \times 10^6$
C1018 Steel	$-(83.1 \pm 4.4) \times 10^6$
Fused Silica	$-(33.2 \pm 0.9) \times 10^6$

It would be interesting to compare the values in Table I with those obtained by other workers but we have been unable to find any third order data on these specific materials.

It has been previously reported[1] that $(\Delta V/V)$ for C1018 steel varies linearly with elastic strain but is relatively insensitive to plastic strain. This result suggests that the dislocation activity, which occurs in the plastic range, must affect V_{S1} and V_{S2} by nearly equal amounts. Thus, $(V_{S1}-V_{S2})$ remains essentially unchanged. The variation of $(\Delta V/V)$ during elastic and plastic deformation has more recently been studied in specimens of 1100-F aluminum. The results have been very similar to those for steel. Figure 2 presents data for a specimen of 1100-F aluminum both before and after yielding. The first data were taken during the initial loading cycle. The specimen was then loaded beyond the yield point until a strain of approximately 0.2 per cent was reached and then the second set of data was taken. The maximum-minimum type pulse echo patterns, which are used in evaluating $(\Delta V/V)$, change continuously as the load varies but they do not appear to vary with time at constant load. However, if the transducer is rotated so that the particle motion is parallel or perpendicular to the compression, an exponential decay pattern is obtained and the attenuation is very time-dependent immediately following load changes. The time-dependent variation in attenuation is apparently due to dislocations that break away from impurities and/or vacancies when the stress is varied. These point defects then diffuse through the lattice and

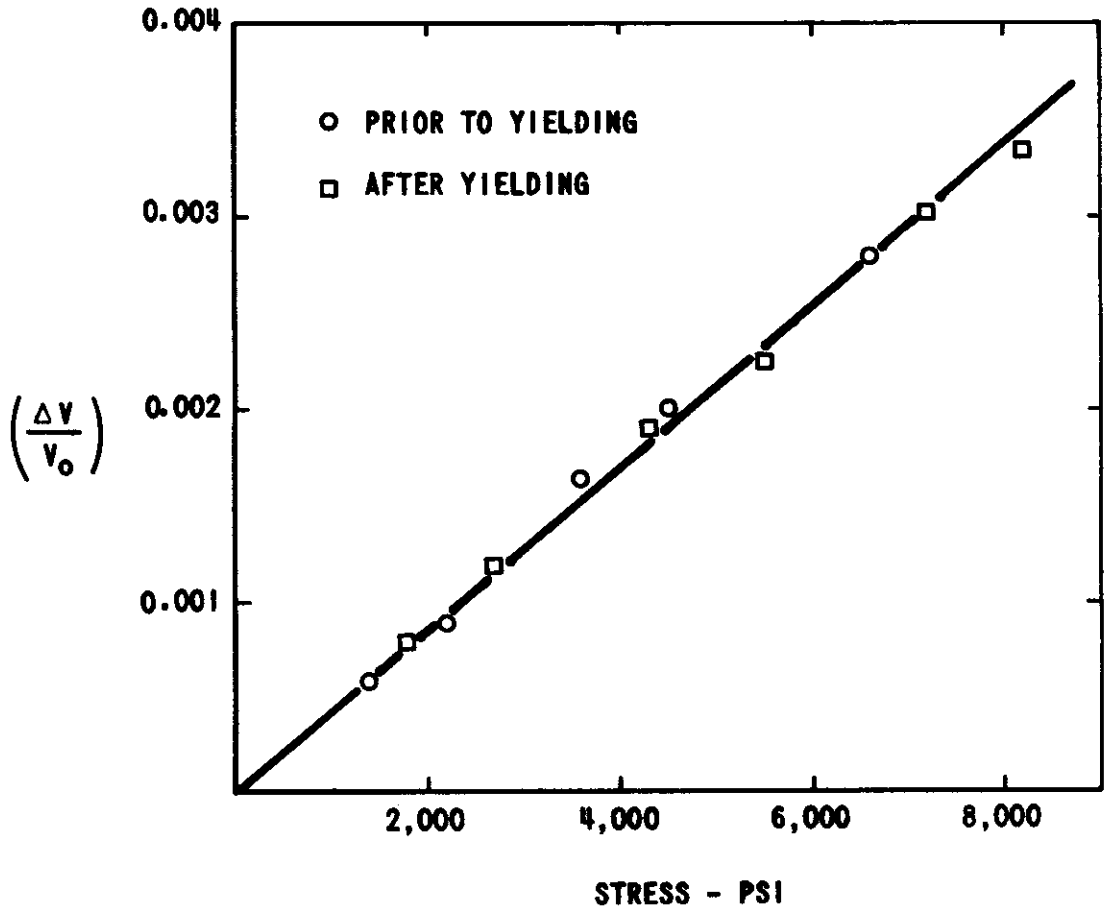

Figure 2 - Stress-Induced Birefringence in 1100-F Aluminum

repin the dislocations as the load is held constant. In contrast, the lack of time dependence in the stress-induced birefringence together with the agreement between pre-yield and post-yield values provide a strong indication that dislocations have little effect on birefringence measurements in polycrystalline steel or aluminum.

We have also studied stress-induced birefringence in single crystals of high purity aluminum and sodium chloride. The results have been similar to those obtained for polycrystalline specimens but somewhat less reproducible. There is an additional effect which one may encounter in working with single crystals and that is internal conical refraction. This effect occurs when shear waves travel through a crystal in a direction that is not exactly parallel to a specific crystal direction. Pure shear waves, for example, can travel through a cubic crystal in the [100] direction and the velocity is independent of the polarization angle. If, however, the propagation direction is slightly misoriented with respect to [100] , then internal conical refraction may occur. Waterman and Teutonico[8] have shown that this effect can produce pulse-echo patterns exactly like those used to evaluate stress-induced anistropy. Precise orientation of the single crystal is very important then in shear wave studies, particularly at high frequencies. The technique of Walker and co-workers[9] was used to orient and grind the mechanical faces of the specimen parallel to a desired crystal face. Subsequent hand lapping was necessary to attain the even more stringent requirements on parallelism between opposite surfaces. For pulse-echo work at frequencies between 10 and 100 mc. the parallelism should be maintained to within 0.00005 in/in.

In addition to the problems outlined above, the single crystal experiments were influenced strongly by dislocation activity. In both aluminum and sodium chloride the shear waves were sent through the crystal along [100] while compressive loads were applied in the [001] direction. As the external stress was applied to aluminum the $(\Delta V/V)$ values were observed to be both stress dependent and time dependent. Upon loading the specimen $(\Delta V/V)$ first increased and then part of the increase was lost as time progressed at constant load. The equilibrium value, reached after a few minutes, was proportional to the applied load. When the load was removed, $(\Delta V/V)$ momentarily increased again, but then decreased with time to the no load value. The equilibrium value after loading, however, was usually higher (indicating increased anisotropy) than prior to loading.

In similar experiments on sodium chloride crystals the $(\Delta V/V)$ values were more reproducible and less time dependent than for aluminum. The variation is probably due to the different slip systems found in the two materials. The primary slip system for aluminum is along (111) planes whereas sodium

chloride slips along (110) planes. For pure shear waves traveling in a [100] direction there is no resolved shear stress across (110) planes but there is a resolved stress across (111) planes. Thus, we see that a [100] shear wave could interact with the many (111) dislocations in aluminum and yet exhibit no interaction with the (110) dislocations in sodium chloride. A change in $(\Delta V/V)$ due to dislocations would only arise, however, from an anisotropic change in the distribution of dislocations. Such anisotropy is highly probable in single crystals where slight changes in the direction of stress application can activate more dislocation activity on some primary slip systems than on others.

III. ULTRASONIC BEAM INTERACTION IN SOLIDS

A. Theory

The nondestructive measurement and analysis of a three-dimensional stress distribution is a difficult problem to contemplate. It is obvious that to succeed in this task one must monitor some property that is stress sensitive and must also localize the volume elements within the test specimen which affect the property being measured. Ultrasonic waves show some promise of being successfully applied to this problem. In addition to certain stress-dependent aspects, ultrasonic waves can be collimated into well defined beams. The intersection of two collimated beams can be used to define a reasonably small volume element within a relatively large metal specimen. Beam interaction or scattering at the point of interaction might be related to stresses at the point of intersection. Whether or not the beam interaction is stress sensitive is secondary, of course, to whether there is a detectable beam interaction at all.

If one considers beam interaction based on linear elasticity theory it is easily shown that the separate waves can each exist independently of the other, i.e., they do not interact. However, if the basic expression of elastic energy is extended to terms cubic in strains the equations of particle motion then contain quadratic terms in the displacements. The independent nature of the intersecting waves no longer holds and the theory admits the possibility of interaction between waves. An analysis of wave interaction in nonlinear solids has been completed during the past year and the results are encouraging. A rather detailed description of the analysis is given in the Appendix so the results will be only briefly summarized here.

The analysis considers the interaction of two waves in a homogenous, isotropic solid. The results indicate that for a given material there does

exist an angle of intersection between two waves of frequencies ω_1 and ω_2 which produces a "resonant" interaction. Under resonant conditions the analysis indicates that scattered waves (with frequencies $\omega_1 \pm \omega_2$) originate at the "point" of intersection. The analysis further predicts the direction of particle motion as well as the propagation direction of the scattered wave. The resonant angles of intersection and the directions of propagation for the scattered waves are summarized in Table II of Appendix I, p. 26.

Some calculations have also been made on the amplitude of the scattered wave. The amplitude is found to be proportional to the volume of interaction and also dependent on the third order elastic constants of the material. A numerical example, based on data for polystyrene, indicates that the displacement amplitude of the scattered wave is not beyond the realm of detection. Nevertheless, the intensity of this wave will undoubtedly be small and optimum conditions must be obtained if detection is to be expected.

B. Preliminary Experiments

Experimental efforts to verify the wave interaction predictions are still in the preliminary stages, but a description of the initial experiment is included here. The only case that has been examined experimentally is the interaction of two transverse waves. From Table II of Appendix I, we see that the scattered wave in this case has a longitudinal mode and a frequency of $(\omega_1 + \omega_2)$. The table also indicates that the angle for resonant interaction is

$$\phi = \arccos\left\{C^2 + \left[(C^2-1)\ (a^2+1)/2a\right]\right\}$$

and that the direction of the scattered wave is $(\vec{K}_1+\vec{K}_2)$. We see, then, that the resonant angle depends only on the transverse to longitudinal velocity ratio, C, and the frequency ratio, a, of the two primary waves. The direction of the scattered wave is determined by the propagation vectors, $\vec{K}_1$ and $\vec{K}_2$, of the primary waves. It is further shown, in the numerical example of Appendix I, that the amplitude of the scattered wave is a maximum when $\omega_1 = \omega_2$. Under these conditions, a wave of frequency 2ω is predicted to emerge in a direction that bisects the angle between the two primary waves. The analysis also indicates that the two primary transverse waves should both be polarized either parallel or perpendicular to the $(\vec{K}_1, \vec{K}_2)$ plane.

A schematic of the interaction experiment described above is shown in Figure 3. The specimen was machined with the shape of an isosceles triangle - the angle between the equal sides being cut so the two primary waves would intersect at the resonance angle, ϕ . The scattered wave should then travel normal to the third side of the triangular specimen. The two transducers used to generate the primary waves were both 5 mc., AC-cut quartz crystals. The receiving transducer was a 10-mc.x-cut crystal. The figure depicts the ultrasonic wave packets after they have passed through the volume of interaction and the scattered wave is just arriving at the receiver crystal. The electrical signal from the crystal is fed to an amplifier tuned for 10 mc., and the amplified signal drives the vertical deflection plates of a cathode ray indicator.

The transmitting crystals were first excited simultaneously with a single 5-mc. signal from one pulse generator. Experiments were also performed using two pulse generators. The two generators were triggered at the same time but the frequency of one could be varied slightly. This procedure was used to possibly compensate for slight errors in both theory and experimental arrangement that could cause the angle ϕ to be in error. The compensation, of course, was expected from changes in the frequency ratio (ω_1/ω_2) which affects the angle, ϕ .

Judicious placement of the three crystals facilitates the detection of the scattered wave by making it possible to distinguish the desired signal from multiple reflections of the primary waves. From simple geometrical considerations, it is easy to calculate the time of travel necessary to bring the primary transverse waves to the intersection zone and the additional time required for the scattered longitudinal wave to travel to the receiver crystal. It is then only necessary to use a scope with a calibrated sweep to localize the desired signal. Multiple reflections of primary waves will arrive at the receiver crystal much later than the scattered wave.

The interaction of two transverse waves has thus far been studied only in fused silica and polycrystalline magnesium. We have not yet been able to detect the predicted longitudinal waves, but several changes are being made to optimize variables and increase sensitivity. An increase in the amplitude of the primary waves and additional amplification of the received signals are possible. Different specimen materials will be investigated to optimize nonlinear parameters. It is also desirable to operate at higher frequencies because the analysis indicates the amplitude of the scattered wave is dependent upon the third power of the primary wave frequency. This factor, of course, must be weighed against the increase in attenuation that occurs at the higher frequencies.

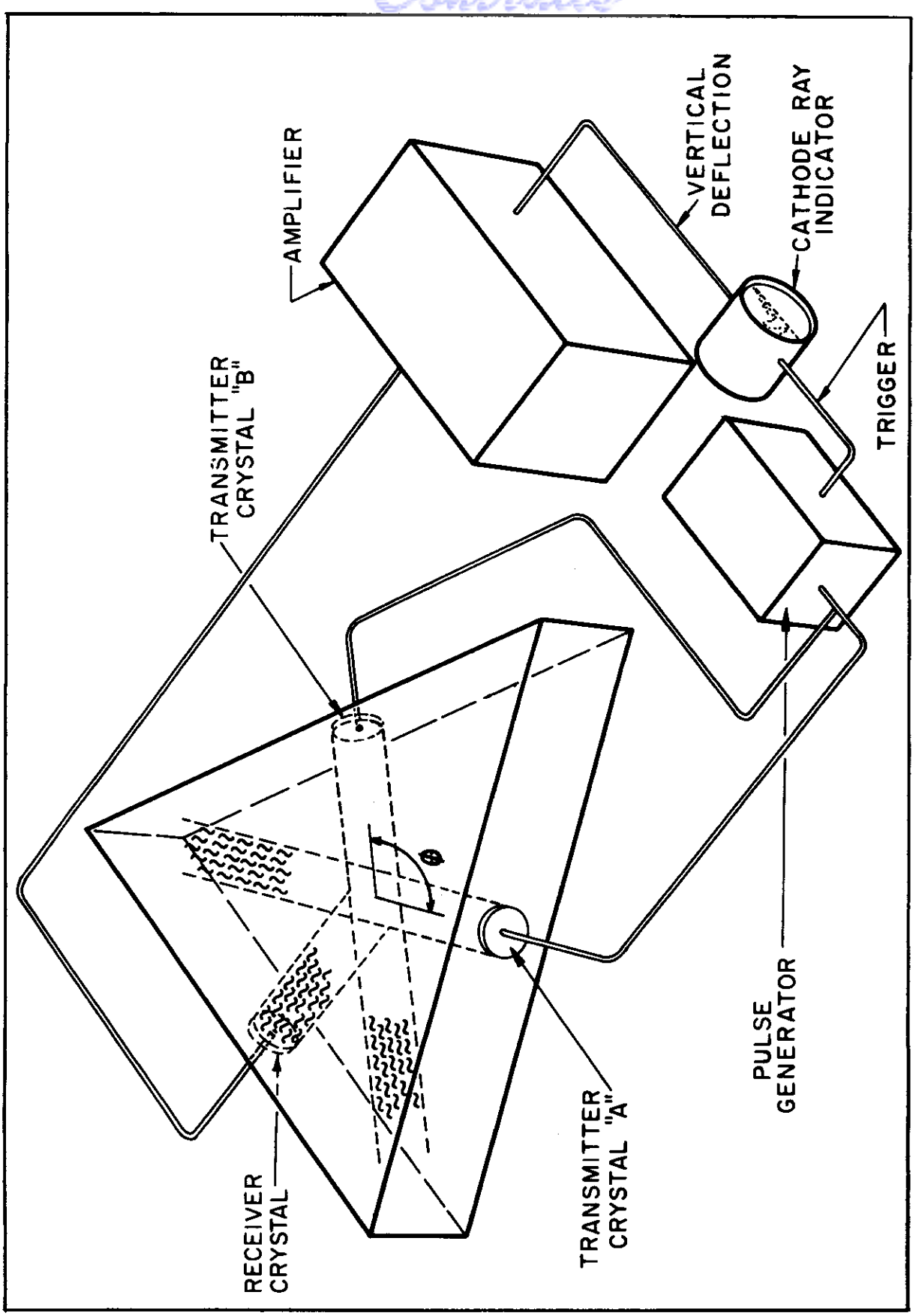

Figure 3 - Schematic of Beam Interaction Experiment

Apparatus is also being assembled for the study of interaction between one transverse wave and one longitudinal wave. This case has one advantage over the transverse-transverse case in that the longitudinal wave can be coupled into solid specimen through a liquid. This makes it much easier to continuously vary the interaction angle, ϕ , and thus optimize the resonant condition. A complete investigation of the interaction phenomena will include numerous experimental arrangements using both pulsed and continuous wave techniques.

IV. SUMMARY

The study of stress-induced birefringence has been continued in both polycrystalline and single crystal experiments. The effect is explained on the basis of nonlinear elasticity theory. Experiments indicate that dislocation activity does not strongly affect results in polycrystalline specimens, however, a pronounced influence may be observed in single crystals.

Nonlinear elasticity theory has also been used to investigate the interaction of two intersecting, plane, elastic waves in a homogeneous, isotropic medium. A criterion for the occurrence of a strong scattered wave has been derived. The criterion is formulated as a relationship between the first-order elastic constants of the material, the angle between the intersecting wave vectors, and the ratio of primary wave frequencies. The amplitude of the scattered wave is found to be proportional to the volume of interaction and dependent on the third order elastic constants of the material. Preliminary efforts to experimentally verify the theoretical predictions are described.

APPENDIX I

THE INTERACTION OF ELASTIC WAVES IN AN ISOTROPIC SOLID

I. INTRODUCTION

In the linear theory of elasticity two elastic waves do not interact. The equations of motion are linear and therefore the principle of superposition holds. Any solution of the equations of motion can be written as a linear combination of monochromatic waves. The linear theory of elasticity results from assuming the elastic energy to be quadratic in the particle displacements. If terms cubic in the particle displacements are included in the elastic energy, the equations of motion become nonlinear.[10] This nonlinearity gives rise to an effective interaction between two plane elastic waves which can produce scattering. The scattering of two collimated, monochromatic, plane waves in an infinite isotropic solid is considered in the present paper.

II. THEORY

When terms cubic in the particle displacements are included in the elastic energy, the resultant nonlinear equations of motion for an isotropic solid are[10]

$$\rho_o \frac{\partial^2 u_i}{\partial t^2} - \mu \frac{\partial^2 u_i}{\partial x_k \partial x_k} - (K+\mu/3) \frac{\partial^2 u_\ell}{\partial x_\ell \partial x_i} =$$

$$(\mu+A/4)\left(\frac{\partial^2 u_\ell}{\partial x_k \partial x_k}\frac{\partial u_\ell}{\partial x_i} + \frac{\partial^2 u_\ell}{\partial x_k \partial x_k}\frac{\partial u_i}{\partial x_\ell} + 2\frac{\partial^2 u_i}{\partial x_\ell \partial x_k}\frac{\partial u_\ell}{\partial x_k}\right)$$

$$+ (K+\mu/3+A/4+B)\left(\frac{\partial^2 u_\ell}{\partial x_i \partial x_k}\frac{\partial u_\ell}{\partial x_k} + \frac{\partial^2 u_k}{\partial x_\ell \partial x_k}\frac{\partial u_i}{\partial x_\ell}\right)$$

$$+ (K-2/3\mu+B)\left(\frac{\partial^2 u_i}{\partial x_k \partial x_k}\frac{\partial u_\ell}{\partial x_\ell}\right) + (A/4+B)\left(\frac{\partial^2 u_k}{\partial x_\ell \partial x_k}\frac{\partial u_\ell}{\partial x_i} + \frac{\partial^2 u_\ell}{\partial x_i \partial x_k}\frac{\partial u_k}{\partial x_\ell}\right)$$

$$+ (B+2C)\left(\frac{\partial^2 u_k}{\partial x_i \partial x_k}\frac{\partial u_\ell}{\partial x_\ell}\right) \qquad (I\text{-}1)$$

where ρ_o = density of the undeformed solid

u_i = i^{th} component of the particle displacement

K = compression modulus

μ = shear modulus.

A , B , and C are third order elastic constants, i.e., they are the coefficients of cubic strain terms in the elastic energy. Subscripts appearing twice in a single term indicate summation over the values 1, 2, 3. The terms x_1 , x_2 , and x_3 are rectangular coordinates.

The left side of Eq. (I-1) is linear in $\vec{u}$ while the right side is quadratic. In practical applications the displacement vector $\vec{u}$ is small and therefore the right side of Eq. (I-1) will be small compared to the left. To solve Eq. (I-1) we set $\vec{u} = \vec{u}^o + \vec{u}^s$ where $\vec{u}^o$ is the solution when the right side of Eq. (I-1) is zero, and $\vec{u}^s$ is a presumably small correction arising from the right-hand side. $\vec{u}_o$ being a solution to the linear equation consists of a superposition of monochromatic waves. Since we are interested in the mutual scattering of two waves we take

$$\vec{u}_o = \vec{A}_o \cos(\omega_1 t - \vec{k}_1 \cdot \vec{r}) + \vec{B}_o \cos(\omega_2 t - \vec{k}_2 \cdot \vec{r}) \quad . \qquad \text{(I-2)}$$

In Eq. (I-2) the amplitude vector may be chosen either parallel or perpendicular to the wave vector $\vec{k}$, that is, the primary waves are either longitudinally or transversely polarized. For a transverse wave $\omega = C_t k$ where $C_t = (\mu/\rho_o)^{\frac{1}{2}}$. For a longitudinal wave $\omega = C_\ell k$ where $C_\ell = \left[(K + 4\mu/3)/\rho_o \right]^{\frac{1}{2}}$.

Now to solve Eq. (I-1) we substitute $\vec{u} = \vec{u}^o + \vec{u}^s$ on the left side and $\vec{u} = \vec{u}^o$ on the right side. This should be a good approximation if $\vec{u}_s$ is small compared to $\vec{u}^o$. Since $\vec{u}^o$ is a solution of the linear equation it disappears from the left side and we obtain

$$\rho_o \frac{\partial^2 u_i^s}{\partial t^2} - \mu \frac{\partial^2 u_i^s}{\partial x_k \partial x_k} - (K + \mu/3) \frac{\partial^2 u_\ell^s}{\partial x_\ell \partial x_i} = p_i \qquad \text{(I-3)}$$

where the vector $\vec{p}$ is determined by putting $\vec{u}_o$ in the right side of Eq. (I-1). If we use Eq. (I-2) for $\vec{u}^o$, $\vec{p}$ will involve a sum of products of two monochromatic waves. Some of the terms will represent the interaction of a primary wave with itself. This interaction has been treated before[10] and we shall not include it here. Including only those terms representing interactions between the primary waves we find for $\vec{p}$ after some tedious manipulation

$$\vec{p}(\vec{r},t) = \vec{I}^{+} \sin\left\{(\omega_1+\omega_2)t-(\vec{k}_1+\vec{k}_2)\cdot\vec{r}\right\} + \vec{I}^{-} \sin\left\{(\omega_1-\omega_2)t-(\vec{k}_1-\vec{k}_2)\cdot\vec{r}\right\} \qquad \text{(I-4)}$$

where

$$\begin{aligned}
\vec{I}^{\pm} = -\tfrac{1}{2}(\mu+A/4)\Big\{&(\vec{A}_o\cdot\vec{B}_o)(\vec{k}_2\cdot\vec{k}_2)\vec{k}_1 \pm (\vec{A}_o\cdot\vec{B}_o)(\vec{k}_1\cdot\vec{k}_1)\vec{k}_2 \\
&+ (\vec{B}_o\cdot\vec{k}_1)(\vec{k}_2\cdot\vec{k}_2)\vec{A}_o \pm (\vec{A}_o\cdot\vec{k}_2)(\vec{k}_1\cdot\vec{k}_1)\vec{B}_o + 2(\vec{A}_o\cdot\vec{k}_2)(\vec{k}_1\cdot\vec{k}_2)\vec{B}_o \\
&\pm 2(\vec{B}_o\cdot\vec{k}_1)(\vec{k}_1\cdot\vec{k}_2)\vec{A}_o\Big\} - \tfrac{1}{2}(K+\mu/3 + A/4 + B)\Big\{(\vec{A}_o\cdot\vec{B}_o)(\vec{k}_1\cdot\vec{k}_2)\vec{k}_2 \\
&\pm (\vec{A}_o\cdot\vec{B}_o)(\vec{k}_1\cdot\vec{k}_2)\vec{k}_1 + (\vec{B}_o\cdot\vec{k}_2)(\vec{k}_1\cdot\vec{k}_2)\vec{A}_o \pm (\vec{A}_o\cdot\vec{k}_1)(\vec{k}_1\cdot\vec{k}_2)\vec{B}_o\Big\} \\
&- \tfrac{1}{2}(A/4+B)\Big\{(\vec{A}_o\cdot\vec{k}_2)(\vec{B}_o\cdot\vec{k}_2)\vec{k}_1 \pm (\vec{A}_o\cdot\vec{k}_1)(\vec{B}_o\cdot\vec{k}_1)\vec{k}_2 + (\vec{A}_o\cdot\vec{k}_2)(\vec{B}_o\cdot\vec{k}_1)\vec{k}_2 \\
&\pm (\vec{A}_o\cdot\vec{k}_2)(\vec{B}_o\cdot\vec{k}_1)\vec{k}_1\Big\} - \tfrac{1}{2}(B+2C)\Big\{(\vec{A}_o\cdot\vec{k}_1)(\vec{B}_o\cdot\vec{k}_2)\vec{k}_2 \\
&\pm (\vec{A}_o\cdot\vec{k}_1)(\vec{B}_o\cdot\vec{k}_2)\vec{k}_1\Big\}
\end{aligned}$$

Since $\vec{p}$ is a known function of $\vec{r}$ and t, Eq. (I-3) is now a linear inhomogeneous equation for the scattered wave $\vec{u}^s$, with $\vec{p}$ acting as a source term. Instead of writing Eq. (I-3) in component form we prefer to use vector notation and write

$$\frac{\partial^2 \vec{u}^s}{\partial t^2}(\vec{r},t) - C_\ell^2 \nabla\left\{\nabla\cdot\vec{u}^s(\vec{r},t)\right\} + C_t^2 \nabla\times\nabla\times\vec{u}^s(\vec{r},t) = 4\pi q(\vec{r},t) \qquad \text{(I-5)}$$

where $4\pi q = \frac{\vec{p}}{\rho_o}$.

This is the standard form for the inhomogeneous vector wave equation.[11] From now on we shall be interested only in the scattered wave sp we shall drop the superscript s until further notice. We introduce the time Fourier transform pairs

$$\vec{u}(\vec{r},\omega) = \int_{-\infty}^{+\infty} e^{i\omega t}\vec{u}(\vec{r},t)dt$$

$$\vec{u}(\vec{r},t) = \frac{1}{2\pi}\int_{-\infty}^{+\infty} e^{-i\omega t}\vec{u}(\vec{r},\omega)d\omega$$

$$\vec{q}(\vec{r},\omega) = \int_{-\infty}^{+\infty} e^{i\omega t}\vec{q}(\vec{r},t)dt$$

$$\vec{q}(\vec{r},t) = \frac{1}{2\pi}\int_{-\infty}^{+\infty} e^{-i\omega t}\vec{q}(\vec{r},\omega)d\omega \qquad . \qquad \text{(I-6)}$$

From Eq. (I-5) the equation for the Fourier transform is

$$-\omega^2\vec{u}(\vec{r},\omega) - C_\ell^2\nabla\left\{\nabla\cdot\vec{u}(\vec{r},\omega)\right\} + C_t^2\nabla\times\nabla\times\vec{u}(\vec{r},\omega) = 4\pi\vec{q}(\vec{r},\omega) \qquad . \qquad \text{(I-7)}$$

From Eq. (I-4) and Eq. (I-6) one finds that

$$\vec{q}(\vec{r},\omega) = \frac{\vec{I}^+}{4i\rho_o}\left\{e^{-i(\vec{k}_1+\vec{k}_2)\cdot\vec{r}}\delta(\omega+\omega_1+\omega_2) - e^{i(\vec{k}_1+\vec{k}_2)\cdot\vec{r}}\delta(\omega-\omega_1-\omega_2)\right\}$$

$$+ \frac{\vec{I}^-}{4i\rho_o}\left\{e^{-i(\vec{k}_1-\vec{k}_2)\cdot\vec{r}}\delta(\omega+\omega_1-\omega_2) - e^{i(\vec{k}_1-\vec{k}_2)\cdot\vec{r}}\delta(\omega-\omega_1+\omega_2)\right\} \qquad \text{(I-8)}$$

where $\delta(\alpha) = 0$ for $\alpha \neq 0$

$\delta(\alpha) = \infty$ for $\alpha = 0$

and

$$\int_{-\infty}^{\infty} \delta(\alpha)d\alpha = 1 \quad .$$

Now Eq. (I-8) is not quite right. We are interested in the case where the primary beams are well collimated. The interaction term $\vec{q}$, which is a product of the amplitudes of the primary beams, will be zero unless we are in the region where the primary beams intersect. We shall denote both the region of intersection and its volume by V. Then Eq. (I-8) is valid only inside V and $\vec{q}$ is zero outside V.

If one assumes that $\vec{u}(\vec{r},\omega)$ decreases at least as fast as $\frac{1}{r}$ for large r, then it can be shown[11] that the solution for Eq. (I-7) in the infinite region can be written as

$$\vec{u}(\vec{r},\omega) = \int_V G(\vec{r},\vec{r}'\omega)\vec{q}(\vec{r}',\omega)dV \qquad \text{(I-9)}$$

where G is a tensor or dyadic operator. For the infinite region, G can be written[11]

$$\vec{\vec{G}}(\vec{r},\vec{r}',\omega) = \frac{1}{C_\ell^2} G_\ell(\vec{r},\vec{r}',\omega/C_\ell) + \frac{1}{C_t^2} G_t(\vec{r},\vec{r}',\omega/C_t) \quad . \qquad \text{(I-10)}$$

In Eq. (I-9) the term arising from G_ℓ will be longitudinal, while the term arising from G_t will be transverse. In dyadic notation G_ℓ and G_t are given by[11]

$$G_\ell(\vec{r},\vec{r}',\omega/C_\ell) = \left[I\left(\frac{1-i\frac{\omega}{C_\ell}R}{\frac{\omega^2}{C_\ell^2}R^2}\right) - \frac{\vec{R}\vec{R}}{R^2}\left(\frac{3-i\frac{\omega}{C_\ell}R-\frac{\omega^2}{C_\ell^2}R^2}{\frac{\omega^2}{C_\ell^2}R^2}\right)\right]\frac{e^{i\frac{\omega}{C_\ell}R}}{R} \quad , \qquad \text{(I-11)}$$

$$G_t(\vec{r},\vec{r}',\omega/C_t) = \left[-I\left(\frac{1-i\frac{\omega}{C_t}R-\frac{\omega^2}{C_t^2}R^2}{\frac{\omega^2}{C_t^2}R^2}\right) + \frac{\vec{R}\vec{R}}{R^2}\left(\frac{3-i\frac{\omega}{C_t}R-\frac{\omega^2}{C_t^2}R^2}{\frac{\omega^2}{C_t^2}R^2}\right)\right]\frac{e^{i\frac{\omega}{C_t}R}}{R} \qquad \text{(I-12)}$$

where $\vec{R} = \vec{r}-\vec{r}'$ (Figure 4) and $R = |\vec{R}|$ and I is the unit dyadic.

We now choose $\vec{r}$ so large that

$$\omega/C_\ell R \gg 1 \ , \ \omega/C_t R \gg 1 \qquad \text{(I-13)}$$

for all $\vec{r}'$ in V. If in addition $|\vec{r}'| \ll |\vec{r}|$ we have

$$R \simeq r-\hat{r}\cdot\vec{r}' \qquad \text{(I-14)}$$

where $\hat{r}$ is a unit vector in the direction of $\vec{r}$, i.e., $\hat{r} = \vec{r}/r$. With these assumptions we can simplify Eq. (I-11) and Eq. (I-12). Firstly, we keep only the leading terms in $(\omega/C_\ell)R$ and $(\omega/C_t)R$. Secondly, we replace R by $r-\hat{r}\cdot\vec{r}'$ in the exponentials and R by r elsewhere. We obtain

$$G_\ell(\vec{r},\vec{r}',\omega/C_\ell) = \hat{r}\hat{r}\,\frac{e^{i\frac{\omega}{C_\ell}r}}{r}\,e^{-i\frac{\omega}{C_\ell}\hat{r}\cdot\vec{r}'} \quad , \qquad \text{(I-15)}$$

$$G_t(\vec{r},\vec{r}',\omega/C_t) = \left[I-\hat{r}\hat{r}\right]\frac{e^{i\frac{\omega}{C_t}r}}{r}\,e^{-i\frac{\omega}{C_t}\hat{r}\cdot\vec{r}'} \quad . \qquad \text{(I-16)}$$

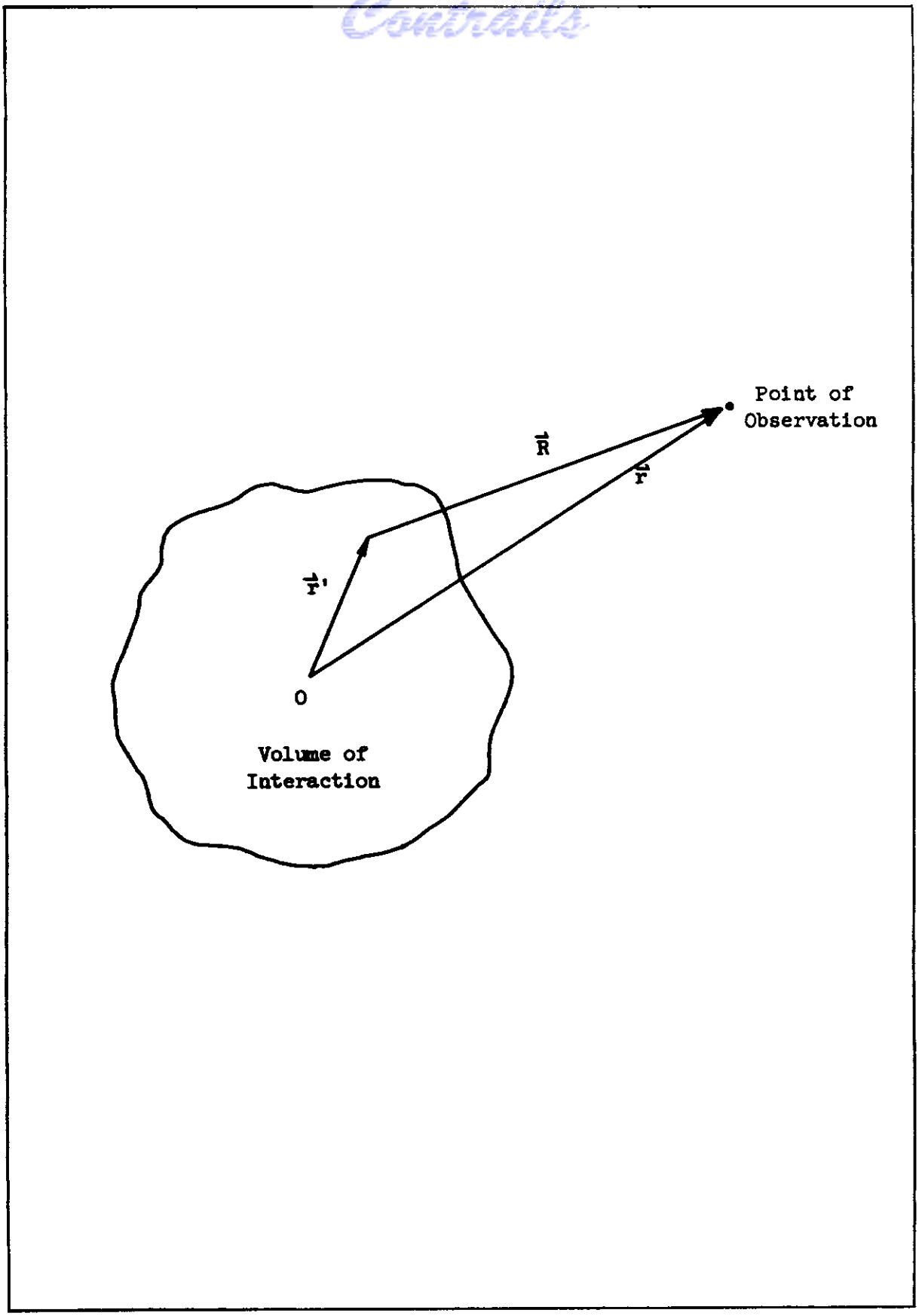

Figure 4 - Vector Arrangement

Now using Eqs. (I-15) and (I-16) in Eq. (I-10) we can find G and using G in Eq. (I-9) with $\vec{q}$ given by Eq. (I-8) we can find $\vec{u}(\vec{r},\omega)$. Then from Eq. (I-6) we can get $\vec{u}(\vec{r},t)$. The result of this straightforward but tedious procedure is

$$\vec{u}(\vec{r},t) = \frac{(\vec{I}^{+}\cdot\hat{r})}{4\pi C_\ell^2\rho_o}\frac{\hat{r}}{r}\int_V \sin\left\{\left(\frac{\omega_1+\omega_2}{C_\ell}\hat{r}-\vec{k}_1-\vec{k}_2\right)\cdot\vec{r}' - (\omega_1+\omega_2)\left(\frac{r}{C_\ell}-t\right)\right\} dV$$

$$+ \frac{(\vec{I}^{-}\cdot\hat{r})}{4\pi C_\ell^2\rho_o}\frac{\hat{r}}{r}\int_V \sin\left\{\left(\frac{\omega_1-\omega_2}{C_\ell}\hat{r}-\vec{k}_1+\vec{k}_2\right)\cdot\vec{r}' - (\omega_1-\omega_2)\left(\frac{r}{C_\ell}-t\right)\right\} dV$$

$$+ \frac{\vec{I}^{+}-(\hat{r}\cdot\vec{I}^{+})\hat{r}}{4\pi C_t^2\rho_o r}\int_V \sin\left\{\left(\frac{\omega_1+\omega_2}{C_t}\hat{r}-\vec{k}_1-\vec{k}_2\right)\cdot\vec{r}' - (\omega_1+\omega_2)\left(\frac{r}{C_t}-t\right)\right\} dV$$

$$+ \frac{\vec{I}^{-}-(\hat{r}\cdot\vec{I}^{-})\hat{r}}{4\pi C_t^2\rho_o r}\int_V \sin\left\{\left(\frac{\omega_1-\omega_2}{C_t}\hat{r}-\vec{k}_1+\vec{k}_2\right)\cdot\vec{r}' - (\omega_1-\omega_2)\left(\frac{r}{C_t}-t\right)\right\} dV \qquad \text{(I-17)}$$

The first and second terms in Eq. (I-17) are longitudinal waves with the summed frequency $\omega_1+\omega_2$ and the difference frequency $\omega_1-\omega_2$, respectively. The third and fourth terms are transverse waves with the summed and difference frequencies, respectively.

The terms in the arguments of the sine function involving $\left(\frac{r}{C}-t\right)$ do not vary during the $\vec{r}'$ integration. Now look at the first term in Eq. (I-17). As we integrate over $\vec{r}'$ the integrand oscillates with frequency determined by the coefficient of $\vec{r}'$, i.e., $\frac{\omega_1+\omega_2}{C_\ell}\hat{r}-\vec{k}_1-\vec{k}_2$ in this case. In general, the result of this integration will depend on just how the waves fit into the region V. As we increase V the value of the integral will oscillate between fixed limits, unless we can find a direction $\hat{r}_s$ for which

$$\frac{\omega_1+\omega_2}{C_\ell}\hat{r}_s-\vec{k}_1-\vec{k}_2 = 0 \quad . \qquad \text{(I-18)}$$

If we can find such an $\hat{r}_s$, the integrand becomes constant for $\hat{r} = \hat{r}_s$ and the amplitude of the scattered wave in this direction becomes proportional to the volume of interaction V. By increasing the volume V one can indefinitely increase the amplitude of the scattered wave in the direction $\hat{r}_s$. In any other direction the amplitude does not increase indefinitely with volume but oscillates. For the proper choice of experimental parameters this will lead to scattering which is sharply peaked in one direction and whose amplitude is proportional to the volume of interaction. We shall call this part of the wave the scattered wave as opposed to the rest of the outgoing wave which has the character of a diffracted wave. Equation (I-18) will be called the resonance condition. We have so far considered only the first term in Eq. (I-17); however, the character of the remaining three terms is the same as that of the first. The resonance conditions for the remaining three terms are, respectively,

$$\frac{\omega_1-\omega_2}{c_\ell}\,\hat{r}_s - (\vec{k}_1-\vec{k}_2) = 0$$

$$\frac{\omega_1+\omega_2}{c_t}\,\hat{r}_s - (\vec{k}_1+\vec{k}_2) = 0$$

$$\frac{\omega_1-\omega_2}{c_t}\,\hat{r}_s - (\vec{k}_1-\vec{k}_2) = 0 \quad .$$

III. INTERACTION CASES

Three cases of interaction between two intersecting waves must be considered, namely,

1. Two transverse waves.

2. Two longitudinal waves.

3. One transverse and one longitudinal wave.

We shall consider the case of two transverse waves in detail by way of example. The results for all three cases are given later in Table II.

For the case of two transverse waves we have

$$\vec{A}_o \cdot \vec{k}_1 = \vec{B}_o \cdot \vec{k}_2 = 0 \quad \text{and} \quad \frac{\omega_1}{C_t} = k_1 \, , \; \frac{\omega_2}{C_t} = k_2 \quad .$$

We want first to see if the resonant condition Eq. (I-18) can be satisfied. We must have

$$\left(\frac{\omega_1+\omega_2}{C_\ell}\right)^2 = k_1^2 + k_2^2 + 2\vec{k}_1 \cdot \vec{k}_2$$

or

$$\left(\frac{\omega_1+\omega_2}{C_\ell}\right)^2 = \frac{\omega_1^2}{C_t^2} + \frac{\omega_2^2}{C_t^2} + \frac{2\omega_1\omega_2}{C_t^2} \cos\varphi$$

where φ is the angle between $\vec{k}_1$ and $\vec{k}_2$. The above leads to

$$\cos\varphi = \frac{C_t^2}{C_\ell^2} + \tfrac{1}{2}\left(\frac{C_t^2}{C_\ell^2} - 1\right)\left(\frac{\omega_1}{\omega_2} + \frac{\omega_2}{\omega_1}\right) \quad .$$

In order that this equation be satisfied we must have the right side less than one and greater than minus one. This leads to the condition that

$$\frac{1-C_t/C_\ell}{1+C_t/C_\ell} < \frac{\omega_1}{\omega_2} < \frac{1+C_t/C_\ell}{1-C_t/C_\ell}$$

For any ω_1/ω_2 in this range we can choose the angle φ between the primary wave vectors $\vec{k}_1$ and $\vec{k}_2$ so that we get a scattered wave (appearing in the direction of $\vec{k}_1+\vec{k}_2$) . If one examines the resonance conditions for the last three terms in Eq. (I-17) it turns out that none of them can be satisfied for this particular choice of primary waves. For the scattered wave then, we have from Eq. (I-17) only the longitudinal wave

$$\vec{u}(\vec{r},t) = \frac{(\vec{I}^{+}\cdot\hat{r}_s)}{4\pi C_\ell^2 \rho_o}\frac{\hat{r}_s}{r} V \sin(\omega_1+\omega_2)(t-r/C_\ell) \quad . \tag{I-19}$$

Using the fact that $\vec{A}_o\cdot\vec{k}_1 = \vec{B}_o\cdot\vec{k}_2 = 0$ in this case we have from Eq. (I-4)

$$\vec{I}^{+} = -\tfrac{1}{2}(\mu+A/4)\left\{(\vec{A}_o\cdot\vec{B}_o)(k_2^2\vec{k}_1+k_1^2\vec{k}_2) + (\vec{B}_o\cdot\vec{k}_1)(\vec{k}_2^2+2\vec{k}_1\cdot\vec{k}_2)\vec{A}_o + (\vec{A}_o\cdot\vec{k}_2)(k_1^2+2\vec{k}_1\cdot\vec{k}_2)\vec{B}_o\right\} - \tfrac{1}{2}(K+\mu/3+A/4+B)(\vec{A}_o\cdot\vec{B}_o)(\vec{k}_1\cdot\vec{k}_2)(\vec{k}_2+\vec{k}_1) - \tfrac{1}{2}(A/4+B)(\vec{A}_o\cdot\vec{k}_2)(\vec{B}_o\cdot\vec{k}_1)(\vec{k}_2+\vec{k}_1) \quad .$$

The amplitude of the scattered wave depends on the polarization of the primary waves. If one primary wave is polarized perpendicular to the $\vec{k}_1,\vec{k}_2$ plane and the other is polarized in the $\vec{k}_1,\vec{k}_2$ plane, then $I^{+}\cdot\hat{r}_s = 0$ and there is no scattered wave even though the resonant condition is met. If both primary waves are polarized perpendicular to the $\vec{k}_1,\vec{k}_2$ plane the scattered wave amplitude is

$$\text{Amp.} = \frac{A_o B_o V\omega_1^3}{16\pi\rho_o r}\left(\frac{1}{C_t^4 C_\ell}\right)\left\{-(\mu+A/4)\left[(a^3+1)(c^2-1)+a(a+1)(c^2+1)\right] - (K+\mu/3+A/4+B)\left[c^2(3c^2-1)(a+a^2)+c^2(c^2-1)(a^3+1)\right]\right\} \tag{I-20}$$

where a is the frequency ratio ω_2/ω_1 and c is the velocity ratio C_t/C_ℓ. If both primary waves are polarized in the $\vec{k}_1,\vec{k}_2$ plane the scattered wave amplitude is similar in form to Eq. (I-20). In fact, the scattered wave amplitudes for all three general interaction cases are of similar form. Since these amplitudes may be obtained from straightforward expansion of the terms in Eq. (I-17), they will not be included in the present paper. The general character of Eq. (I-20) will be discussed in a later section.

It remains to consider the case where both primary waves are longitudinal, and the case where one is longitudinal and one transverse. Complete results are given in Table II. For the case of two longitudinal waves, the

TABLE II

INTERACTION CASES WHICH PRODUCE A SCATTERED WAVE

Primary Waves	Resonant Wave Type and Frequency	Direction of Scattered Wave	$\cos\varphi$ *	Frequency Limits/
Two transverse	Longitudinal $(\omega_1+\omega_2)$	$\vec{k}_1+\vec{k}_2$	$c^2+\left[(c^2-1)(a^2+1)/2a\right]$	$\frac{1-c}{1+c} < a < \frac{1+c}{1-c}$
Two longitudinal	Transverse $(\omega_1-\omega_2)$	$(\vec{k}_1-\vec{k}_2)/(\omega_1-\omega_2)$	$1/c^2+\left[(c^2-1)(a^2+1)/2ac^2\right]$	$\frac{1-c}{1+c} < a < \frac{1+c}{1-c}$
One longitudinal and one transverse#	Longitudinal $(\omega_1+\omega_2)$	$\vec{k}_1+\vec{k}_2$	$c+\left[a(c^2-1)/2c\right]$	$0 < a < \frac{2c}{(1-c)}$
One longitudinal and one transverse#	Longitudinal $(\omega_1-\omega_2)$	$(\vec{k}_1-\vec{k}_2)/(\omega_1-\omega_2)$	$c+\left[a(1-c^2)/2c\right]$	$0 < a < \frac{2c}{1+c}$
One longitudinal and one transverse#	Transverse $(\omega_1-\omega_2)$	$(\vec{k}_1-\vec{k}_2)/(\omega_1-\omega_2)$	$1/c+\left[(c^2-1)/2ac\right]$	$\frac{1-c}{2} < a < \frac{1+c}{2}$

* φ is the angle between $\vec{k}_1$ and $\vec{k}_2$ at resonance.
a is the frequency ratio ω_2/ω_1.
c is the velocity ratio C_t/C_ℓ.

/ When a is within the limits shown, it is possible to choose an angle φ that will give a scattered wave.

\# The frequency of the longitudinal primary wave is ω_1.

resonant condition can be satisfied for the fourth term of Eq. (I-17) only. For the remaining case the resonant conditions can be satisfied for the first, second, and fourth terms. In this latter case of interaction between a longitudinal and a transverse primary wave, the amplitude of the longitudinal scattered waves vanish when $\vec{B}_o$ is polarized perpendicular to the plane of $\vec{k}_1, \vec{k}_2$. The transverse scattered wave has finite amplitude for any polarization of $\vec{B}_o$.

The appearance, in Table II, of scattered waves with the difference frequency $\omega_1-\omega_2$ requires some comment. Treatment of the interaction problem has been on a strictly classical basis in this paper. The classical treatment is an approximation to the correct Quantum Mechanical treatment. A macroscopic plane elastic wave consists of the presence of a very large number of phonons of a particular (long) wavelength in the crystal. With this in mind one can do the following calculations:

1. Write down the phonon Hamiltonian for the crystal including the first term giving phonon-phonon interaction.

2. Assume that at $t = 0$, there are a large number of phonons with wave vectors $\vec{k}_1$ and $\vec{k}_2$ and energies $\hbar\omega_1$, $\hbar\omega_2$.

3. Assume that first order time dependent perturbation theory is valid and compute the state of the system at some time t_1 later than $t = 0$.

If one does this calculation the following points appear. Due to the structure of the phonon-phonon interaction there is conservation of the phonon wave vector (no Umklapp processes are possible if the initial wavelengths are very long). That is, a phonon of wave vector k_1 and one of wave vector $\vec{k}_2$ can produce, in interaction, only phonons of wave vector $\vec{k}_3 = \vec{k}_1+\vec{k}_2$. The second point is that if t_1 is not chosen too small, the perturbation theory gives only energy conserving transitions, that is, we must also have $\hbar\omega_3 = \hbar\omega_2+\hbar\omega_1$. These conditions on the wave vector and energy taken together are equivalent to the resonance condition from Eq. (I-18). A troublesome point is, however, that this calculation seems to indicate that a scattered wave with the difference of the primary frequencies cannot arise, in contrast to the classical calculation which permits a scattered wave of either the sum or difference frequencies. It is therefore not clear to us whether or not the difference frequency waves will actually be produced in an experiment. Since the validity of the assumptions made in both calculations is somewhat of an open question, it is difficult to make a more definite statement at the present time.

IV. BEAM WIDTH OF SCATTERED WAVE

The scattered wave given by Eq. (I-17) appears in the form of a conical beam with vertex at the interaction zone and maximum intensity along the direction of the vector $\hat{r}_s$. In experiments aimed at detecting the scattered wave it would be advantageous to minimize the spread of this beam. The parameters which determine the angular width of the beam may be identified as follows.

Consider the first term in the right-hand side of Eq. (I-17). The amplitude of the integral is equal to the volume of interaction V when $\hat{r} = \hat{r}_s$. We seek here the vector $\hat{r}_o$ for which the amplitude first becomes zero (or a minimum) as $\hat{r}$ moves away from $\hat{r}_s$. This occurs when one full cycle of the wave is fitted into V , or in other words, when the coefficient of $\vec{r}'$ is approximately equal $2\pi/\ell$, ℓ being a length characterizing the volume of interaction. It follows that the angular width of the beam is proportional to λ_s/ℓ where λ_s is the wavelength of the scattered wave. Thus the scattered beam will be narrow when $\lambda_s \ll \ell$. For the case we are considering λ_s is inversely proportional to $\omega_1+\omega_2$ so the width of the scattered beam may be made small by using large primary frequencies and/or a large interaction volume.

When the other terms in Eq. (I-17) are considered, the same proportionality to λ_s/ℓ is obtained. However, for the second and fourth terms, λ_s is inversely proportional to $\omega_1-\omega_2$ which suggests that in general a scattered wave with the difference frequency will be more spread out.

V. NUMERICAL EXAMPLE

We use a numerical example to illustrate the previous results. Choosing polystyrene for the elastic medium we have[3]

$$\lambda = 2.89 \times 10^{10} \text{ dynes/cm}^2$$

$$\mu = 1.38 \times 10^{10} \text{ dynes/cm}^2$$

$$K = 3.81 \times 10^{10} \text{ dynes/cm}^2$$

$$A^* = -1.00 \times 10^{11} \text{ dynes/cm}^2$$

$$B = -8.3 \times 10^{10} \text{ dynes/cm}^2$$

$$C = -1.06 \times 10^{11} \text{ dynes/cm}^2$$

$$\rho_o = 1.056 \text{ gm/cm}^3$$

Taking again the case of two transverse primary waves we find that resonance can be obtained for

$$0.338 < a < 2.955 \quad .$$

Since the two primary waves are the same type, we may without loss of generality choose $\omega_1 > \omega_2$ which restricts a to the range

$$0.338 < a \leq 1 \quad .$$

The smallest angle φ between the primary waves for which a scattered (resonant) wave is obtained is 120.8 degrees corresponding to $a = 1$. As a decreases, φ approaches 180 degrees.

If both primary waves are polarized perpendicular to the $\vec{k}_1, \vec{k}_2$ plane, the scattered wave amplitude Eq. (I-20) is largest for $a = 1$. We then obtain

$$\text{Amp. (max.)} = 10.32 \times 10^{-18} A_o B_o V \omega_1^3 / r \text{ cm.}$$

(when A_o, B_o, and r are in centimeters, V in cubic centimeters and ω_1 in radians/sec). As a decreases, the amplitude passes through a minimum at $a \approx 0.583$ and we find that

$$\text{Amp.(min.)} = 7.45 \times 10^{-18} A_o B_o V \omega_1^3 / r \text{ cm.}$$

---

* The correlation between the elastic constants ℓ, m, and n given in Ref. 3 and A, B, and C used here is: $A = n$, $B = m - \frac{1}{2}n$, $C = \ell - m + \frac{1}{2}n$.

Clearly, the amplitude is more sensitive to the primary wave frequencies characterized by ω_1, than to the frequency ratio.

Let us further evaluate the interaction in polystyrene of two 10-megacycle waves with a volume of intersection equal to 1 cm^3. If the displacement amplitude of the interacting waves is approximately 10^{-10} cm. and we let r = 10 cm., then the displacement amplitude of the scattered wave is calculated to be approximately 10^{-15} cm. By maintaining the same volume, frequency, and observation distance, we see that the amplitude of the scattered wave varies as the product of the primary wave amplitudes. Thus, the difference between the amplitudes of the primary waves and the scattered wave decreases as A_o and B_o get larger. If we use the unreasonably large value of 10^{-6} cm. for A_o and B_o (this corresponds to a strain amplitude of about 10^{-3} in the above example), then we find that the amplitudes of the intersecting and scattered waves are of the same order of magnitude.

VI. CONCLUSIONS

Two intersecting plane elastic waves produce a scattered wave when the resonant condition (Eq. (I-18)) is satisfied. The resonant condition is a function of the ratio of the primary frequencies but is independent of the absolute frequencies. The scattered wave appears in the approximate form of a conical beam emanating from the volume of interaction and has maximum intensity along the direction $\hat{r}_s$ defined by the resonant condition. The width of the beam is proportional to λ_s/ℓ where λ_s is the wavelength of the scattered wave and ℓ is a length characterizing the volume of interaction V. The maximum intensity of the scattered wave is greatest for high primary frequencies, large primary wave amplitudes, and large interaction volume.

In an experiment aimed at detecting the scattered wave, the distance L from the interaction zone to the point of observation should be large compared with ℓ. Therefore, optimum experimental conditions are

$$L \gg \ell \gg \lambda_s$$

BIBLIOGRAPHY

1. F. R. Rollins, "Ultrasonic Methods for Nondestructive Measurement of Residual Stress," WADD TR 61-42, Part I (1961).

2. F. D. Murnaghan, "Finite Deformations of an Elastic Solid" (John Wiley & Sons, Inc., New York, 1951).

3. D. S. Hughes and J. L. Kelly, Phys. Rev., 92, 1145 (1953).

4. A. Seeger and O. Buck, Z. Naturforschung, 15a, 1056 (1960).

5. T. Bateman, W. P. Mason, and H. J. McSkimen, J.A.P. 32, 928 (1961).

6. A. Granato and K. Lücke, J.A.P., 27, 583 (1956).

7. A. Granato and K. Lücke, J.A.P., 27, 589 (1956).

8. P. C. Waterman and L. J. Teutonico, J.A.P., 28, 266 (1957).

9. J. G. Walker, H. J. Williams, and R. M. Bozorth, Rev. of Scientific Instruments, 20, 947 (1949).

10. Z. A. Goldberg, Soviet Physics Acoustics, 6, 306 (1961).

11. P. M. Morse and H. Feshback, "Methods of Theoretical Physics," Part II, Chap. 13 (McGraw-Hill Book Co., Inc. 1953).